Size-tuneable and micro-patterned iron nanoparticles derived from biomolecules via microcontact printing SAM-modified substrates and controlled-potential electrolyses

Masato Tominaga,* Katsuya Miyahara, Kazuki Soejima, Shinya Nomura, Manabu Matsumoto and Isao Taniguchi*

Graduate School of Science and Technology, Kumamoto University,

Kumamoto 860-8555, Japan

[*] Corresponding author:

Masato Tominaga

e-mail: masato@gpo.kumamoto-u.ac.jp

Tel.: +81-96-342-3656, Fax: +81-96-342-3656

Abstract

Site-selected and size-controlled iron nanoparticles were prepared on coplanar surfaces via microcontact printing of SAM-modified Au/mica electrodes and controlled-potential electrolytic reactions using ferritin biomolecules.

Ferritin molecules packed like a full monolayer on 6-amino-1-hexanethiol (AHT)- and 11-amino-1-undecanethiol (AUT)-modified Au/mica surface via electrostatic interactions, which did not depend on the chain length of the amino terminal alkane thiols. After heat-treatment at 400 ˚C for 60 min, iron oxide nanoparticles (ca. 5 nm in diameter) derived from ferritin cores were observed at the Au/mica surface by atomic force microscopy (AFM).

On the study on the electrochemistry of ferritin immobilized onto ATH- and AUT-modified Au/mica electrodes, the redox response of the ferritin immobilized AHT-modified electrode was clearly observed. On the other hand, no redox peak for ferritin was obtained at the AUT-modified electrode. The electron transfer between ferritin and the electrode through the AHT membrane could not take place. The difference in the electrochemical response of ferritin immobilized onto AUT- and AUT-modified Au/mica was caused by the chain length of the amino terminal alkane thiols.

Uniform patterns of AHT and AUT on the Au/mica electrode surface were performed by use of a poly-(dimethylsiloxane) (PDMS) stamp. After the immobilization of ferritin onto both AHT- and AUT-modified electrode surfaces, the modified electrode was applied to a -0.5 V potential for 30 min in a phosphate buffer solution. After this procedure, the PDMS stamp patterning image appeared by scanning electron microscopy (SEM) image. The SEM results induced by the size change of the ferritin core consisting of iron(III) by electrolysis.

keywords: ferritin; pattern; nanoparticles; iron oxide; electrolysis

1. Introduction

Size-tuneable preparations and patterning of metallic nanoparticles have been widely studied because metallic nanoparticles are of particular interest in many applications. Many kinds of

strategies developed to prepare metallic nanoparticles such as the use of block copolymer thin films, ink-jet printing, photolithography and scanning probe microscopy-based lithographies [1-3]. In particular, the microcontact printing method which uses a poly-(dimethylsiloxane) (PDMS) stamp is simple and useful [3]. However, it is still a challenge to fabricate and pattern diameter controlled nanoparticles on a surface.

The formation of solids in biological systems, biomineralization, has provided inspiration for the controlled formation of inorganic materials [4,5]. Ferritin, an iron-storage protein, is a potential candidate for the protein engineering of nanomaterial syntheses [6-19]. The iron uptake and release mechanisms of ferritin are caused by the oxidation and reduction of iron ions, Fe(II/III), in the protein shell [6-11]. The structure of the ferritin core is $(FeOOH)_8(FeOPO_3H_2)$, which is a ferrihydrite phosphate. The inner and outer diameters of the protein shell are ca. 6 and 12 nm, respectively [6-11]. Recently, the formation of nanoparticles consisting of inorganic species such as cobalt, nickel, chromium, copper, indium and Prussian blue in the ferritin cavity have been reported [20-24]. Furthermore, iron nanoparticles derived from ferritin cores have been used as catalysts in carbon nanotube syntheses [25,26]. In the present study, we demonstrate that size-tuneable and micro-patterned iron nanoparticles derived from ferritin via the microcontact printing of a SAM-modified substrate and controlled-potential electrolysis can be prepared. The results obtained herein demonstrate one possible solution for the size-tuneable preparation and patterning of metallic nanoparticles. Uniformly patterned size-controlled iron nanoparticles on the coplanar surface can be used as catalysts for the chemical vapour deposition growth of diameter-controlled carbon nanotubes with diameter control via the iron nanoparticle size.

2. Materials and methods

Horse spleen ferritin (Type I, Sigma) was purified by size exclusion chromatography [6]. The concentration of purified ferritin was determined by BCA-protein reactions (BCA protein assay kit, PIERCE Chem. Comp., USA) against a bovine serum albumin standard curve [27]. The number of iron atoms per ferritin molecule used in this study was evaluated to be approximately 3 x 10^3 atoms by inductively coupled plasma-atomic emission and atomic absorption spectroscopies. The following SAMs were used without further purification: 6-amino-1-hexanethiol (AHT, 90%, Dojin Chem. Co., Japan) and 11-amino-1-undecanethiol (AUT, 90%, Dojin Chem. Co.). The gold thin film substrate was prepared on mica (Au/mica) by the vapor deposition of 100 nm of gold (99.999% purity) onto freshly cleaved mica sheets (Nilaco Co., Japan) at a reduced pressure, < 0.1 x 10^{-6} Torr. The temperature of the mica sheet was maintained at 350 ˚C during the vapor deposition. The cyclic voltammograms of the Au/mica surface observed in the 0.01 mol dm^{-3} $HClO_4$ solution indicated that the gold surface was enriched with Au(111) facets [28]. The atomically flat nature of the prepared Au/mica surface was identified by atomic force microscopy (AFM).

The Au/mica surface was modified with the AHT and AUT SAMs according to methods described in previous papers [26,29]. The AHT and AUT covering the surface of the Au/mica electrode was estimated to be 7.5 ($\pm$ 0.2) x 10^{-10} mol cm^{-2} by voltammograms in a 0.5 M KOH solution, indicating that a full coverage monolayer had been formed on the gold surface [30]. To immobilize ferritin on the AHT- and AUT-modified electrode surfaces, modified Au/mica electrodes were immersed into a phosphate buffer solution (pH 7, μ = 0.1) of 2 μmol dm^{-3} ferritin for 60 min. Prior measuring, the electrode surface was gently rinsed with buffer. Water was purified with a Millipore Milli-Q water system. Other reagents used in this study were of analytical grade. Tapping-mode AFM measurements were carried out under an air atmosphere using standard silicon

cantilevers. Cyclic voltammetric measurements and controlled-potential electrolyses were performed with an electrochemical analyzer (ALS/Chi, Model 600A) in a conventional three electrode cell with Ag/AgCl (saturated KCl) as the reference electrode and a Pt plate as the counter electrode.

3. Results and discussion

Fig. 1 shows AFM images of ferritin molecules immobilized onto the AHT- and AUT-modified Au/mica surface. The size of each ferritin molecule was evaluated to be approximately 11 (± 1.5) nm in diameter in z-plane thickness, which is comparable to the expected ~12 nm diameter determined by x-ray diffraction [6-11]. These results indicate that ferritin molecules pack like a full monolayer, which dose not depend on the chain length of the amino terminal alkane thiols. It is well known that an electrostatic interaction between a protein and an electrode surface is the key factor of importance in immobilizing the protein onto an electrode surface. The isoelectric point of horse spleen ferritin has been reported to be 4.1 – 5.1 [31], indicating that the whole ferritin molecule has a negative charge in the buffer solution (pH 7) used. Therefore, it is expected that ferritin was immobilized onto the AHT- and AUT-modified electrodes by electrostatic interactions between the ferritin molecule and the amino terminal group of AHT and AUT. After heat-treatment at 400 ˚C for 60 min, nanoparticles (ca. 5 nm in diameter) derived from ferritin cores were observed at the Au/mica surface as shown in Fig. 1b, d. X-ray photoelectron spectroscopy (XPS) results for nanoparticles on the surface showed broad peaks around 712 eV corresponding to iron species. This result taken together with those from previous reports indicate that the observed nanoparticles were FeOOH iron oxides [32,33]. The complete elimination of both the polypeptide of ferritin and SAMs

was identified by reflection absorbance IR spectra and XPS results. The obtained iron nanoparticles act as catalysts for carbon nanotube syntheses as described in detail elsewhere [25,26].

The electrochemistry of ferritin immobilized onto a SAM-modified Au/mica electrode was carried out, as shown in Fig. 2a. The redox response of the ferritin immobilized AHT-modified electrode was clearly observed around -0.3 V. On the other hand, no redox peak for ferritin was obtained at the AUT-modified electrode, even though ferritin was immobilized on the AUT-modified electrode as shown in Fig. 2b. The electron transfer between ferritin and the electrode through the AHT membrane could not take place. The difference in the electrochemical response of ferritin immobilized onto AUT- and AUT-modified Au/mica was caused by the chain length of the amino terminal alkane thiols, which would be useful for preparing patterning nanoparticles with different sizes on coplanar substrates, as described below.

Uniform patterns of AHT and AUT on the Au/mica electrode surface were performed by use of a poly-(dimethylsiloxane) (PDMS) stamp as shown in Fig. 3. First, an ethanol solution of 1 mmol dm^{-3} AUT was applied to the stamp by covering the stamp with the AUT solution using a pipet and then dried under atmospheric conditions. The AUT was then transferred onto the surface of Au/mica by bringing the stamp into conformal contact with the substrate for 1 min. After the PDMS stamp was peeled off, the surface was rinsed with ethanol to remove excessive AUT molecules. Next, the Au/mica partially modified with AUT was immersed into a water solution of 1 mmol dm^{-3} AHT for 3 min. The immobilization of ferritin onto both AHT- and AUT-modified electrode surfaces was carried out by immersing the SAM-modified electrode into a phosphate buffer solution (pH 7) with 2 μmol dm^{-3} ferritin for 60 min. Fig. 4a shows the scanning electron microscopy (SEM) image of the ferritin immobilized AHT- and AUT-modified patterning surface. No patterning image was observed. Next, the modified electrode was applied to a -0.5 V potential for 30 min in a

phosphate buffer solution. After this procedure, the PDMS stamp patterning image appeared by SEM, as shown in Fig. 4b. The SEM results would be anticipated if the size change of the ferritin core consisting of iron(III) had occurred by electrolysis. In other words, iron(III) in ferritin core was reduced to iron(II), and then the reduced iron(II) was released from the protein shell, which resulted in a smaller core size than that observed before electrolysis.

To confirm the reduction of iron and subsequent release as outlined above, the ferritin core size was evaluated before and after electrolysis. The electrolysis at -0.5 V for 30 min was carried out at a ferritin immobilized AHT-modified electrode. The size of each ferritin molecule was evaluated to be approximately 11 (± 1.5) nm in diameter in z-plane thickness with AFM measurements, which was the same in size as ferritin before the electrolysis. After the ferritin immobilized electrode was heat-treated at 400 ˚C for 60 min, iron oxide nanoparticles were observed at its surface. The size distribution of iron oxide nanoparticles before and after the electrolysis is also shown in Fig. 5a,b. The nanoparticles were evaluated to be 1.25 (± 0.5) nm in diameter. The aforementioned result indicates that reduced iron(II) ions were released and ferritin core sizes decreased in comparison to those prior to electrolysis. On the other hand, when the AUT-modified electrode was used, on the other hand, no change in the iron oxide nanoparticles size was observed (Fig. 5c,d). These results clearly indicate that size- and site-controlled iron nanoparticles can be prepared by conjugating methods such as electrolysis and PDMS stamp patterning of SAMs with ferritin.

In conclusion, we demonstrated that site-selected and size-controlled iron nanoparticles can be prepared on a coplanar surface via PDMS stamping and controlled-potential electrolytic reaction using ferritin. The results obtained herein support the possibility of carbon nanotube syntheses with selected positions and controlled diameters on coplanar substrate surfaces.

Acknowledgments

We greatly appreciate professor Marc D. Porter, Ames Laboratory-USDOE, Iowa State University and professor C.-J. Zhong, State University of New York for generously supplying the PDMS stamp. This work was partially supported by a Grant-in-Aid for Scientific Research (M.T.) from the Ministry of Education, Culture, Science, Sports and Technology, Japan. M.T. also acknowledges the Asahi Glass Foundation.

References

[1] G. A. Ozin and A. C. Arsenault, Nanochemistry: A Chemical Approach to Nanomaterials, RSC Publishing, Cambridge, 2005; V. Rotello, Nanoparticles: Building Blocks for Nanotechnology, Kluwer Academic/Plenum Publishers, New York, 2004; F. Caruso, Colloids and Colloid Assemblies, Wiley-VCH Verlag GmbH, Weinheim, Germany, 2004; G. Decher and J. B. Schlenoff, Multilayer Thin Films: Sequential Assembly of Nanocomposite Materials, Wiley-VCH Verlag GmbH, Weinheim, Germany, 2003.

[2] R. A. Segalman, Mater. Sci. Eng., R48 (2005) 191, ; C. M. Welch and R. G. Compton, Anal. Bioanal. Chem., 384 (2006) 601.

[3] R. M. Nyffenegger and R. M. Penner, Chem. Rev., 97 (1997) 1195, ; B. L. Cushing, V. L. Kolesnichenko and C. J. O'Connor, Chem. Rev., 104 (2004) 3893; B. D. Gates, Q. Xu, M. Stewart, D. Ryan, C. G. Willson and G. M. Whitesides, Chem. Rev., 105 (2005) 1171; J. C. Love, L. A. Estroff, J. K. Kriebel, R. G. Nuzzo and G. M. Whitesides, Chem. Rev., 105 (2005)

1103; Y. Xia and G. M. Whitesides, Angew. Chem., Int. Ed. Engl., 37 (1998) 550; Y. Xia and G. M. Whitesides, Annu. Rev. mater. Sci., 28 (1998) 153; M. Geissler and Y. Xia, Adv. Mater., 16 (2004) 1249.

[4] T. Douglas and M. Young, Nature, 393 (1998) 152.

[5] T. Douglas, in: S. Mann (Ed.), Biomimetic Materials Chemistry, Wiley, New York, 1996.

[6] P. M. Harrison and T. H. Lilley, in: T. M. Loehr (Ed.), Iron Carriers and Iron Proteins, VCH Press, New York, 1989, Ch. 2.

[7] T. G. St. Pierre, P. Chan, K. R. Bauchspiess, J. Webb, S. Betteridge, S. Walton and D. P. E. Dickson, Coord. Chem. Rev., 151 (1996) 125.

[8] P. M. Proulx-Curry and N. D. Chasteen, Coord. Chem. Rev., 144 (1995) 347.

[9] G. D. Watt, R. B. Frankel and G. C. Papaefthymiou, Proc. Natl. Acad. Sci., 82 (1985) 3640.

[10] P. M. Harrison, P. J. Artymiuk, G. C. Ford, D. M. Lawson, J. M. A. Smith, A. Treffry and J. L. White, in: S. Mann, J. Webb and R. J. P. Williams (Eds.), Biomineralization Chemical and Biochemical Perspectives, Wiley-VCH Press, Weinheim, Germany, 1989, Ch. 9.

[11] X. Liu and E. C. Theil, Acc. Chem. Res., 38 (2005) 167.

[12] T. Douglas, E. Strable, D. Willits, A. Aitouchen, M. Libera and M. Yound, Adv. Mater. 14 (2002) 415.

[13] M. Allen, D. Willits, J. Mosolf, M. Young and T. Douglas, Adv. Mater., 14 (2002) 1562.

[14] S. C. Tsang, J. Qiu, P. J. F. Harris, Q. J. Fu and N. Zhang, Chem. Phys. Lett., 322 (2000) 553.

[15] J.-M. Bonard, P. Chauvin and C. Klinke, Nano Lett., 6 (2002) 665.

[16] Y. Zhang, Y. Li, W. Kim, D. Wang and H. Dai, App. Phys. A, 74 (2002) 325.

[17] H.-A. Hosein, D. R. Strongin, M. Allen and T. Douglas, Langmuir, 20 (2004) 10283.

[18] . Okuda, Y. Kobayashi, K. Suzuki, K. Sonoda, T. Kondoh, A. Wagawa, A. Kondo and H. Yoshimura, Nano Lett., 5 (2005) 991.

[19] S. Yoshii, K. Yamada, N. Matsukawa and I. Yamashita, Jpn. J. Appl. Phys., 144 (2005) 1518.

[20] T. Douglas and V. T. Stark, Ionrg. Chem., 39 (2002) 1828.

[21] M. Okuda, K. Iwahori, I. Yamashita and H. Yoshimura, Biotech. Bioeng., 84 (2003) 187.

[22] J. M. Dominguez-Vera and E. Colacio, Inorg. Chem., 42 (2003) 6983.

[23] D. Ensign, M. Young and T. Douglas, Inorg. Chem., 43 (2004) 3441.

[24] M. Tominaga, L. Han, L. Wang, M. M. Maye, J. Luo, N. Kariuki and C. J. Zhong, J. Nanosci. Nanotech., 4 (2004) 708.

[25] Y. Li, W. Kim, Y. Zhang, M. Rolandi, D. Wang and H. Dai, J. Phys. Chem. B, 105 (2001) 11424.

[26] M. Tominaga, A. Ohira, A. Kubo, I. Taniguchi, M. Kunitake, Chem. Commun. (2004) 1518.

[27] P. K. Smith, R. I. Krohn, G. T. Hermanson, A. K. Mallia, F. H. Gartner, M. D. Provenzano, E. K. Fujimoto, N. M. Goeke, B. J. Olson and D. C. Klenk, Anal. Biochem., 150 (1985) 76.

[28] K. Uosaki, Y. Shen and T. Kondo, J. Phys. Chem., 99 (1995) 14117.

[29] M. Tominaga, A. Ohira, Y. Yamaguchi and M. Kunitake, J. Electroanal. Chem., 566 (2004) 323.

[30] C. A. Widrig, C. Chung and M. D. Porter, J. Electroanal. Chem., 310 (1991) 335.

[31] P. Arosio, T. G. Adellman, J. W. Drysdale, J. Biol. Chem. 253 (1978) 4451.

[32] I. Yamashita, Thin Solid Films, 393 (2001) 12.

[33] T. Hikono, Y. Uraoka, T. Fuyuki and I. Yamashita, Jpn. J. Appl. Phys., 42 (2003) L398.

Figure captions

Fig. 1. Tapping-mode AFM images before (a, c) and after (b, d) heat treatment at 400 ˚C for 60 min for ferritin immobilized onto AHT (a, b) and AUT (c, d) -modified Au/mica substrates.

Fig. 2. Typical cyclic voltammograms for ferritin immobilized onto AHT (a) and AUT (b) -modified Au/mica electrodes in a phosphate buffer solution (pH 7). Potential sweep rate: 50 mV s^{-1}. Cyclic voltammograms of AHT- and AUT-modified Au/mica electrodes are shown as broken lines. Electrode area: 0.25 cm^{-2}.

Fig. 3. Schematic illustration of the patterning procedures for AHT and AUT, and modification of ferritin molecules on surfaces.

Fig. 4. SEM images for ferritin immobilized onto micro patterning surface by AHT and AUT before (a) and after (b) potential-controlled electrolyses.

Fig. 5. Tapping-mode AFM images for iron oxide nanoparticles derived from heat treatment for ferritin immobilized onto AHT (a, b) and AUT (c, d) –modified Au/mica substrates before (a, c) and after (b, d) potential-controlled electrolyses, and their size distribution. Cross-sectional views correspond to the lines drawn.

5: Figure 1
Click here to download high resolution image

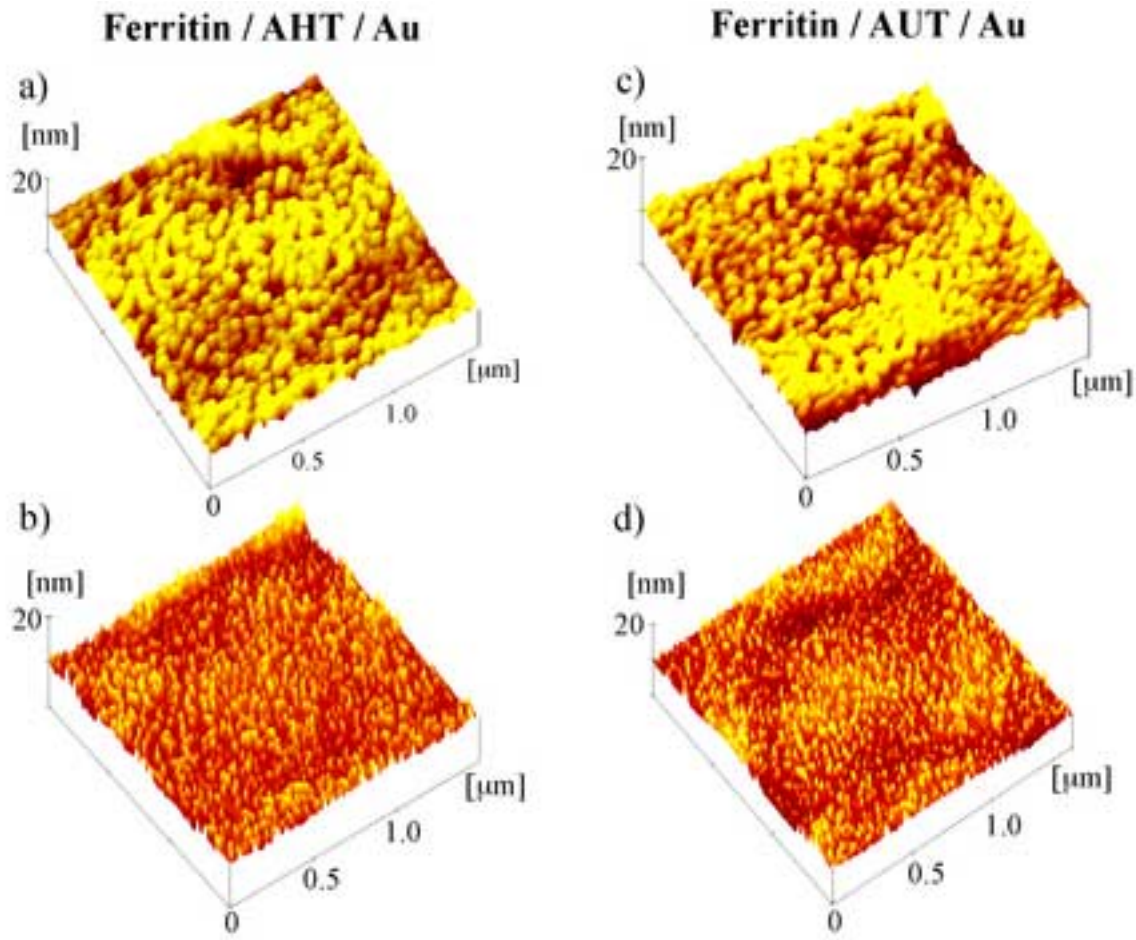

Fig. 1

5: Figure 2
Click here to download high resolution image

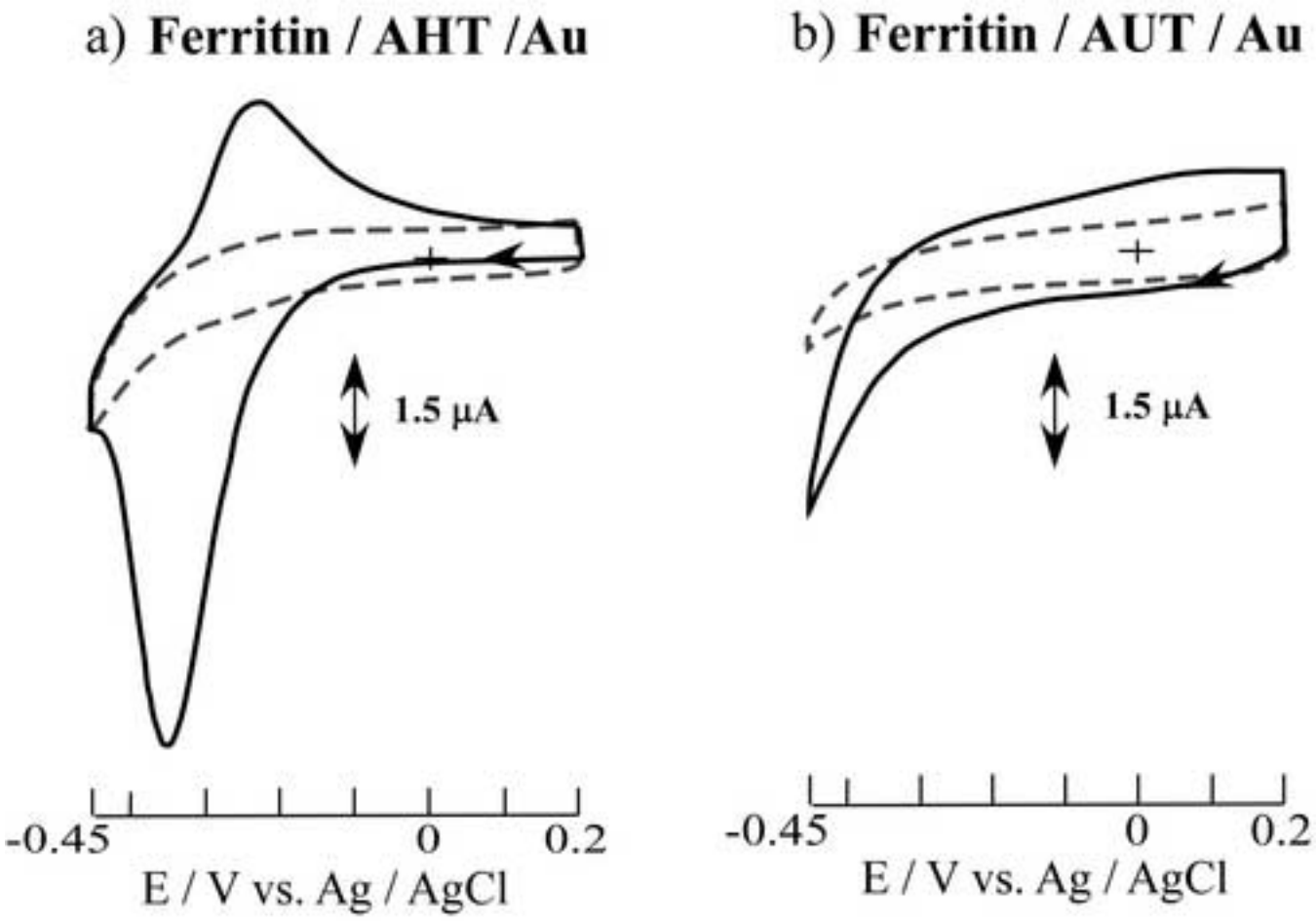

Fig. 2

5: Figure 3
Click here to download high resolution image

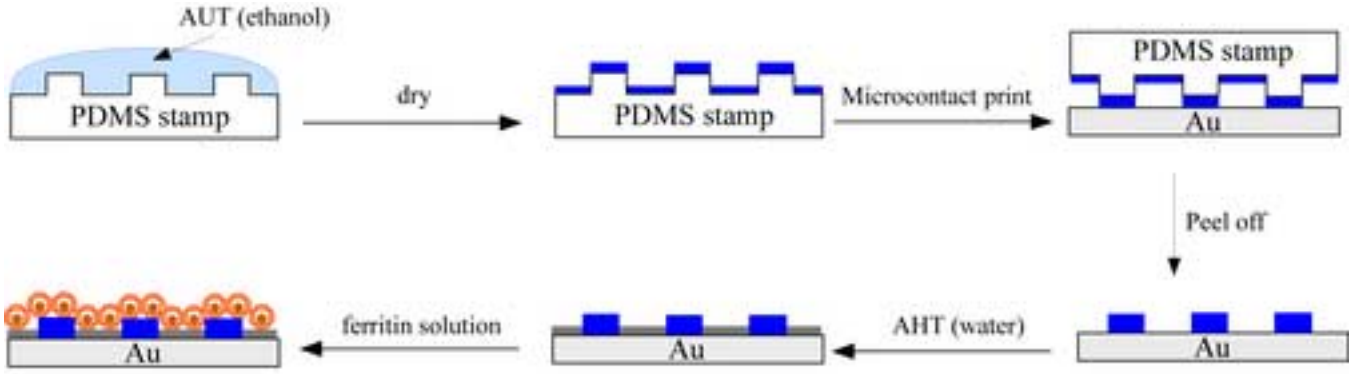

Fig. 3

5: Figure 4
Click here to download high resolution image

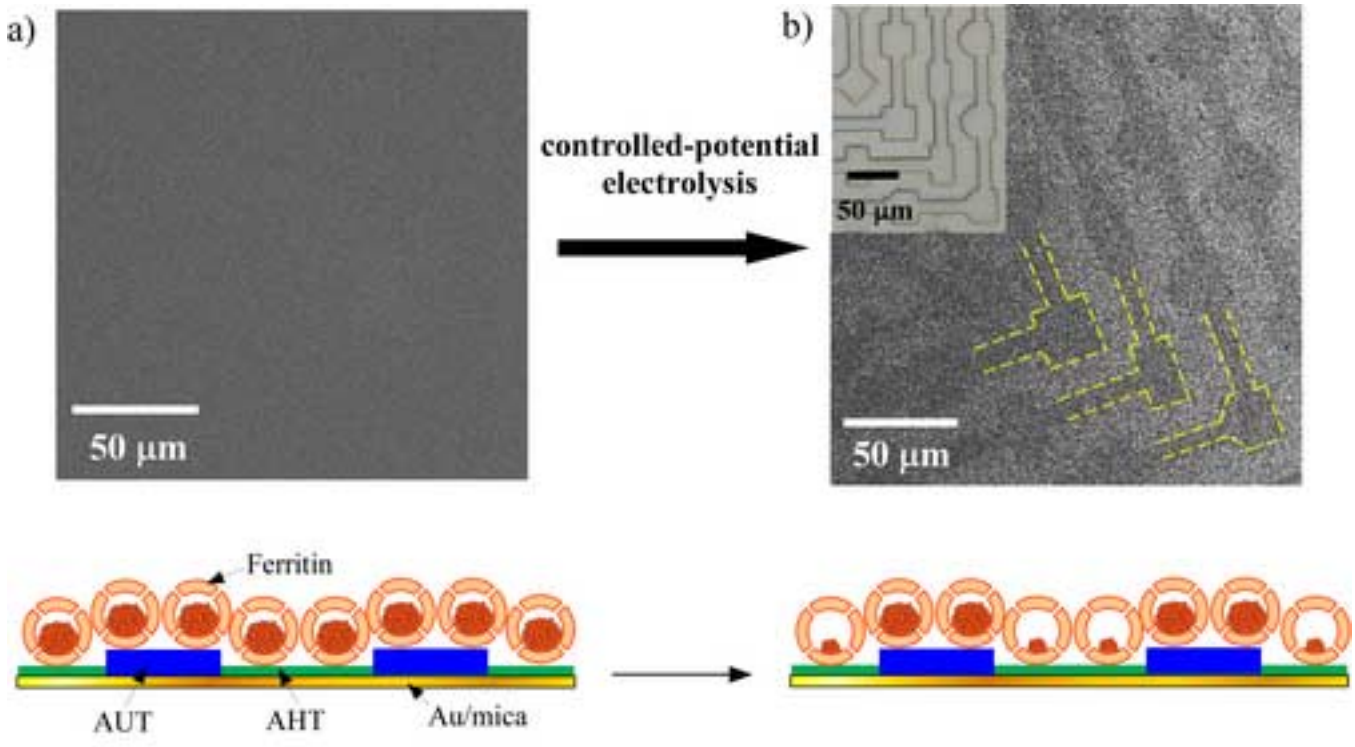

Fig. 4

5: Figure 5

Click here to download high resolution image

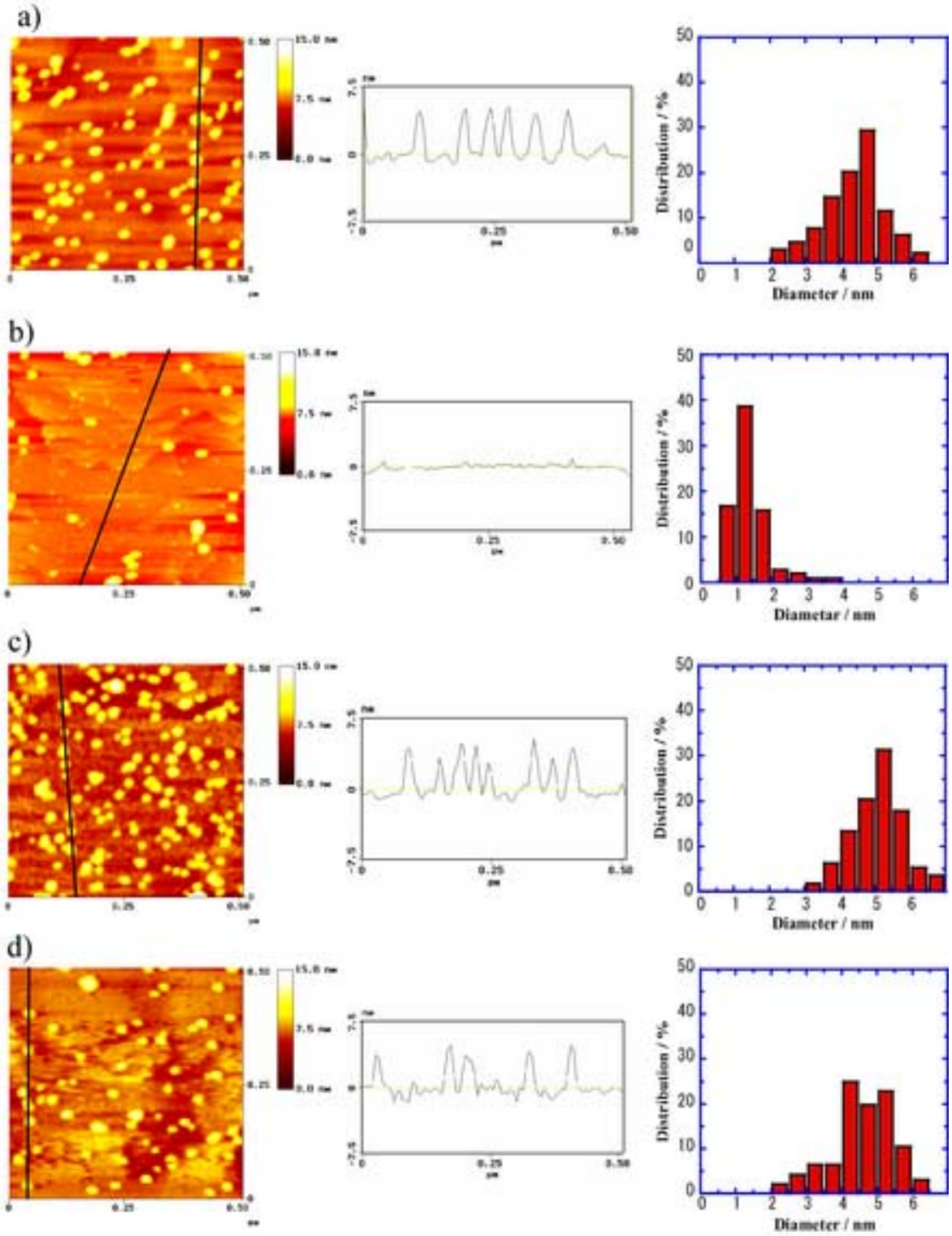

Fig. 5